Observational Validation of Layer-lifting Metrics of Convective Instability for Determining the Dissipation of Severe MCSs

Diego A. Alfaro[1] and Michael C. Coniglio[2]

[1]Center of Atmospheric Sciences, National Autonomous University of Mexico | [2]NOAA/OAR/National Severe Storms Laboratory

1. Background

Layer-lifting indices measure the latent-heating achievable by all inflowing parcels in forward-propagating MCSs, contemplating both the instability of air at low-levels and the dilution produced by mid-level inflow (Fig. 1; see Alfaro 2017). Motivated by potential applications to forecasting MCS maintenance, we evaluate the effectiveness of layer-lifting indices for discriminating between mature and dissipating MCSs. Based on Alfaro and Coniglio (2018), hereafter AC18.

$$\mathrm{CAPE}_{\parallel} = \left(\int_0^{z_{tr}} \rho\,|u_{env} - \mathrm{PS}|\,\mathrm{CAPE}\,dz\right) \times \left(\int_0^{z_{tr}} \rho\,|u_{env} - \mathrm{PS}|\,dz\right)^{-1}$$

$$\mathrm{ICAPE} = \int \rho(z)\mathrm{CAPE}(z)\,dz$$

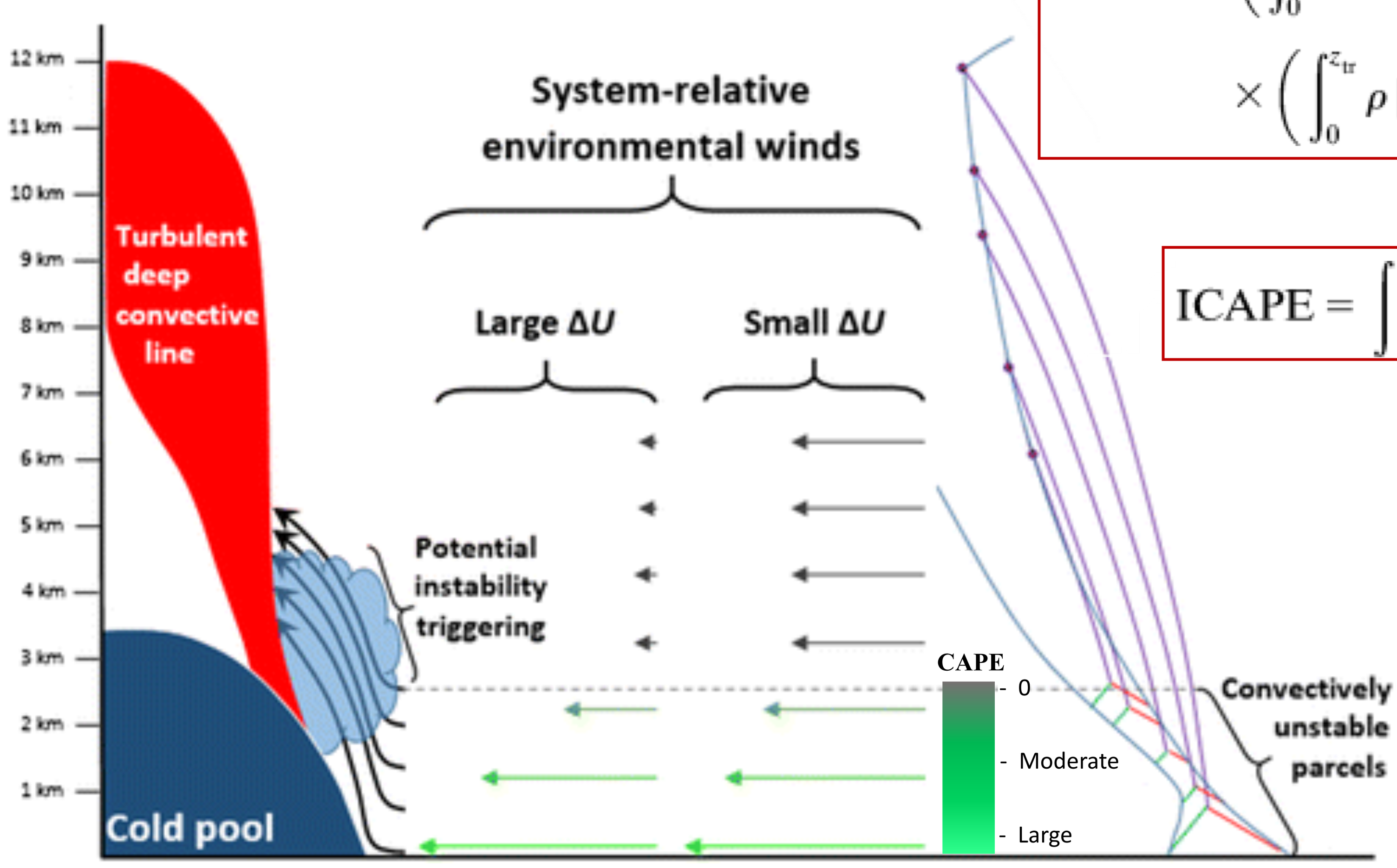

Figure 1. Layer-lifting ascent produced by the cold pool. The potential latent-heating by all unstable parcels is measured by integrated CAPE (ICAPE). Layer-lifting CAPE ($\mathrm{CAPE}_{\parallel}$) is an inflow-weighted mean CAPE, wherein greater inflow of stable mid-level air (gray arrows) causes greater dilution of buoyancy. Small Δ*U* produces greater inflow of mid-level air, implying lower $\mathrm{CAPE}_{\parallel}$. From Alfaro (2017).

2. Methods

Radar reflectivity plots were used to subjectively identify 131 severe, linear and forward-propagating MCSs during the warm season over the continental US (2010-2014). Times and locations of maturity and dissipation were determined to specify the MCS's environment at each stage (Fig. 2). Relevant environmental metrics were computed from RUC/RAP analysis data (Table), excluding precipitating grid-points. Following Coniglio et al. (2007), non-parametric statistical analyses (Wilcoxon signed-rank test) were used to determine a metric's ability to discriminate between stages.

MCS reaches maturity: intense leading line and broad region of stratiform precipitation

MCS dissipation begins: weaker reflectivity in leading line and reduced stratiform region

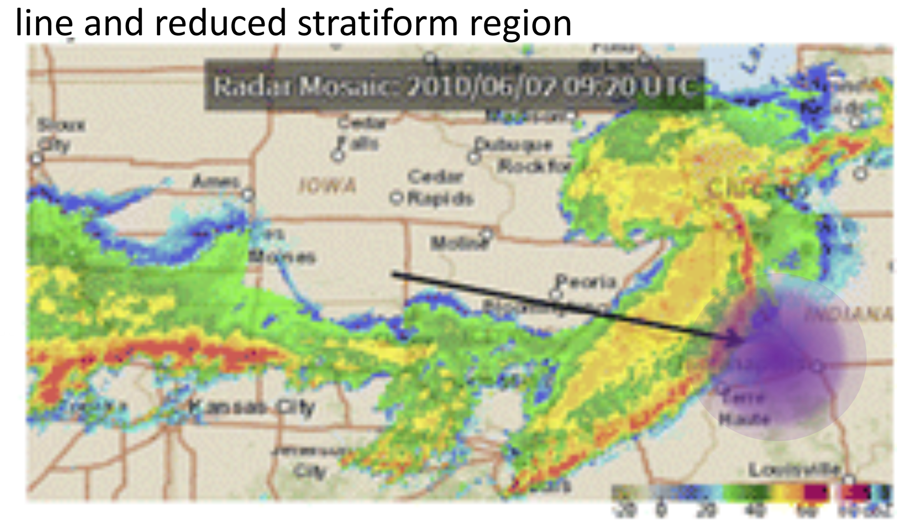

Figure 2. Radar reflectivity of mature (top) and dissipating (bottom) MCS. Arrow shows the MCS's movement. Purple area is the MCS's environment. From AC18.

Thermodynamic/hybrid metrics	Kinematic Metrics
$\mathrm{CAPE}_{\parallel}$	IF_3
ICAPE	$\mathrm{IF}_{4.5}$
MLCAPE	IF_6
MUCAPE	$\mathrm{SVM}_{0\text{-}3}$
PW	$\mathrm{SVM}_{0\text{-}6}$
$\mathrm{PW}_{0\text{-}2}$	$\mathrm{SVM}_{0\text{-}9}$
$\mathrm{PW}_{2\text{-}6}$	$\overline{\mathrm{Wind}}_{0\text{-}3}$
$\mathrm{LR}_{0\text{-}1.5}$	$\overline{\mathrm{Wind}}_{3\text{-}6}$
$\mathrm{LR}_{0\text{-}3}$	$\overline{\mathrm{Wind}}_{0\text{-}9}$
$\mathrm{LR}_{1.5\text{-}6}$	$\mathrm{MPar\_}\overline{\mathrm{Wind}}_{0\text{-}3}$
$\mathrm{LR}_{3\text{-}6}$	$\mathrm{MPar\_}\overline{\mathrm{Wind}}_{3\text{-}6}$
Logit_CBWC (Coniglio et al. 2007)	$\mathrm{MPar\_}\overline{\mathrm{Wind}}_{3\text{-}9}$
	$\mathrm{MPar\_Shear}_{0\text{-}3}$
	$\mathrm{MPar\_Shear}_{3\text{-}6}$
	$\mathrm{MPar\_Shear}_{3\text{-}9}$
	$\mathrm{MPerp\_}\overline{\mathrm{Wind}}_{0\text{-}3}$
	$\mathrm{MPerp\_}\overline{\mathrm{Wind}}_{3\text{-}6}$
	$\mathrm{MPerp\_}\overline{\mathrm{Wind}}_{3\text{-}9}$
	$\mathrm{MPerp\_Shear}_{0\text{-}3}$
	$\mathrm{MPerp\_Shear}_{3\text{-}6}$
	$\mathrm{MPerp\_Shear}_{3\text{-}9}$

IF_x -> Inflow Fraction of air below x km to total inflow (dilution)
LR -> Lapse Rate
PW -> Precipitable Water
MPar -> Motion-parallel
MPerp -> Motion-perpendicular
SVM -> Shear Vector Magnitude
$\overline{\mathrm{Wind}}$ -> Mean wind over the layer indicated by the subscript

Table. Environmental metrics under consideration. Subscripts denote layer (in km) where metric is computed.

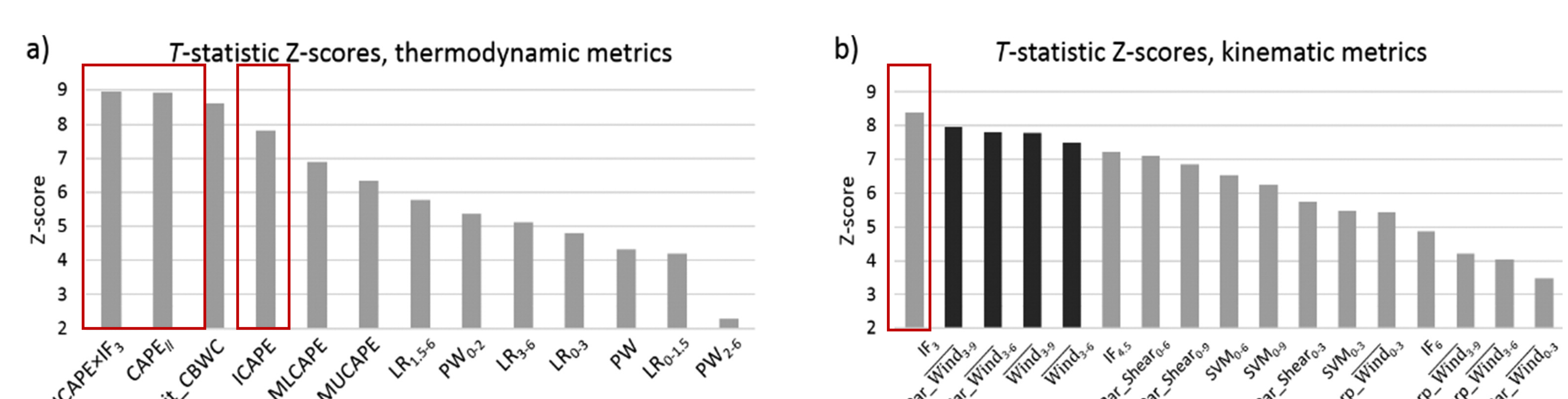

Figure 3. T-statistic Z-scores for metrics that reached 0.05 statistical significance. Dark bars indicate metrics that tend to decrease in value as MCSs dissipate. Red rectangles indicate layer-lifting indices. From AC18.

3. Results

Figure 3 shows Z-scores attained by all metrics. Higher Z-scores imply greater skill to discriminate MCS stage. Layer-lifting metrics $\mathrm{CAPE}_{\parallel}$, ICAPE, IF_3 (measuring dilution due to kinematics) and $\mathrm{ICAPExIF}_3$ are among the most skillful discriminators. Mid-tropospheric inflow ($\mathrm{MPar\_}\overline{\mathrm{Wind}}$) has high Z-score due to impacts on buoyancy dilution (Fig. 1). The skillfulness of $\mathrm{CAPE}_{\parallel}$ is revealed in Fig. 4 by the small overlap between mature and dissipating populations, and the difference in mean/median. Nearly identical results were obtained when estimating MCS movement with Corfidi vectors (not shown; see AC18), paving the way for applying $\mathrm{CAPE}_{\parallel}$ to guide MCS maintenance forecasts.

Standardized distribution of best performing metrics

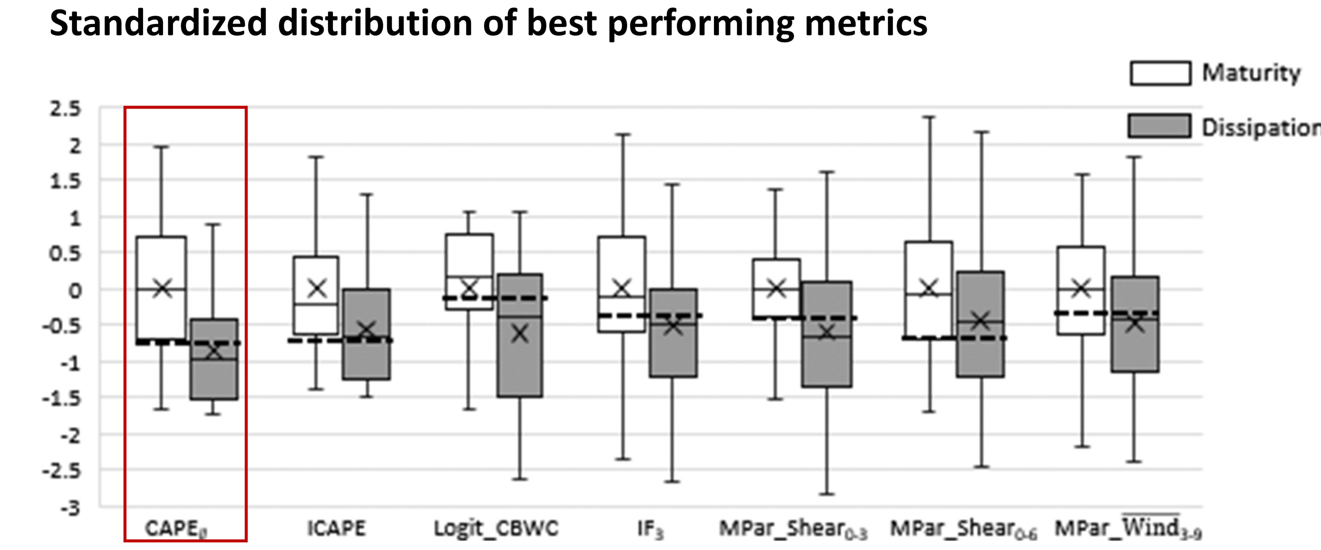

Figure 4. Box-whisker plot of standardized metrics at maturity and dissipation, showing mean (cross), median (solid line) and optimal discriminating threshold (dashed line). From AC18.

4. Conclusions

Diminishing layer-lifting convective instability appears to be a primary driver of MCS dissipation, complementing numerical analyses by Alfaro (2017) showing that MCS intensity is mainly dependent on layer-lifting latent heating. $\mathrm{CAPE}_{\parallel}$ could provide valuable information to forecasters, e.g. helping reduce the false alarm rate.

Alfaro, D. A., 2017: Low-Tropospheric Shear in the Structure of Squall Lines: Impacts on Latent Heating under Layer Lifting Ascent. *J. Atmos. Sci.*, **74**, 229-248.
Alfaro, D. A., and M. C. Coniglio, 2018: Discrimination of Mature and Dissipating Severe-Wind-Producing MCSs with Layer-Lifting Indices. Wea. Forecasting, 33, 3–21.
Coniglio, M. C., H. E. Brooks, S. J. Weiss, and S. F. Corfidi, 2007: Forecasting the maintenance of quasi-linear mesoscale convective systems. *Wea. Forecasting*, **22**, 556-570.